Structural Engineering and Mechanics, *Vol. 69, No. 6 (2019) 693-698*
DOI: https://doi.org/10.12989/sem.2019.69.6.693

Closed-form solution of axisymmetric deformation of prestressed Föppl-Hencky membrane under constrained deflecting

Yong-Sheng Lian[1], Jun-Yi Sun*[1,2], Jiao Dong[1], Zhou-Lian Zheng[1,2a] and Zhi-Xin Yang[1]

[1]School of Civil Engineering, Chongqing University, Chongqing 400045, PR China
[2]Key Laboratory of New Technology for Construction of Cities in Mountain Area (Chongqing University), Ministry of Education, Chongqing 400045, PR China

(Received May 3, 2018, Revised January 26, 2019, Accepted February 5, 2019)

Abstract. In this study, the problem of axisymmetric deformation of prestressed Föppl-Hencky membrane under constrained deflecting was analytically solved and its closed-form solution was presented. The small-rotation-angle assumption usually adopted in membrane problems was given up, and the initial stress in membrane was taken into account. Consequently, this closed-form solution has higher calculation accuracy and can be applied for a wider range in comparison with the existing approximate solution. The presented numerical examples demonstrate the validity of the closed-form solution, and show the errors of the contact radius, profile and radial stress of membrane in the existing approximate solution brought by the small-rotation-angle assumption. Moreover, the influence of the initial stress on the contact radius is also discussed based on the numerical examples.

Keywords: circular membrane; axisymmetric deformation; constrained deflecting; uniformly loading; closed-form solution

1. Introduction

Membrane structures and membrane components play increasingly important roles in many fields. For instance, in the micro-electro-mechanical system, the diaphragm membrane is an important component of the pressure sensor (Molla-Alipour and Ganji 2015, Lian *et al.* 2017a), and in the thin-film-substrate system, the mechanical parameters of thin films are determined based on the deflection of the membrane (Sun *et al.* 2011, 2014, Todorovic *et al.* 2014, Yang *et al.* 2018). So, the analytical solutions of membrane problems are usually needed in many applications. But, in fact, the large deflection phenomena of membrane problem usually give rise to some intractable nonlinear equations which are difficult to be analytically solved (Chucheepsakul *et al.* 2009, Ersoy *et al.* 2009, Sun *et al.* 2010, Hasheminejad and Ghaheri 2015). Therefore, the analytical solutions of membrane problems are available in a few cases.

One hundred years ago, Hencky (1915) originally dealt with the problem of axisymmetric deformation of Föppl-Hencky membrane, i.e., the peripherally fixed circular membrane under the action of uniformly-distributed transverse loads (Arthurs and Clegg 1994, Sun *et al.* 2013), and presented a power series solution. A computational error in Hencky (1915) was corrected by Chien (1948) and Alekseev (1953), respectively. This solution is usually called well-known Hencky solution for short, and is often referred to or cited in a number of related studies (Weinitschke 1973, Beck and Grabmuller 1992, Feng *et al.* 2015, Yang *et al.* 2017). Sun *et al.* (2015) presented the extended Hencky solution, which is applicable to membranes with or without initial stress, but it is still a solution with the small-rotation-angle assumption of membrane. Recently, the well-known Hencky problem was resolved and its closed-form solution was presented, in which the so-called small-rotation-angle assumption of membrane, i.e., the slope angle θ of membrane is so small that the condition $\sin\theta \approx \tan\theta$ could approximately hold, was given up (Lian *et al.* 2016, 2017b).

In this study, we will focus on the analytical processing of an interesting novel membrane problem, the problem of axisymmetric deformation of prestressed Föppl-Hencky membrane under the combined action of uniformly-distributed transverse loads and horizontal frictionless rigid plate, where the case before contact between membrane and horizontal frictionless rigid plate is exactly the well-known Hencky problem, and the horizontal plate actually acts as a limiting deflection of membrane (constrained deflecting). This membrane problem comes from the touch mode capacitive pressure sensors. Recently, Wang *et al.* (2018) dealt with this problem, but the initial stress in membrane was not taken into account and the so-called small-rotation-angle assumption of membrane was still adopted. However, the initial tension is very easy to be present in the initially flat membrane. And the so-called small-rotation-angle assumption of membrane will inevitably bring computational error no matter how small the slope angle θ of membrane is, moreover, the analytical solution obtained by the so-called small-rotation-angle assumption will no

*Corresponding author, Professor
E-mail: sunjunyi@cqu.edu.cn
[a]Professor

ISSN: 1225-4568 (Print), 1598-6217 (Online)

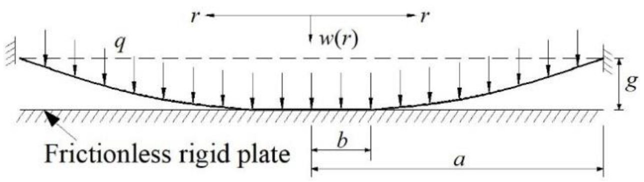

Fig. 1 Sketch of confined deformation of the uniformly loaded circular membrane

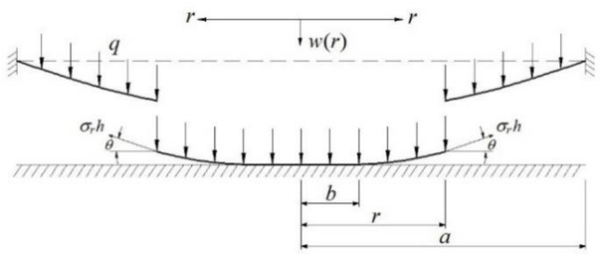

Fig. 2 The equilibrium diagram of the central portion ($b \le r \le a$) of the circular membrane

longer apply when the applied transverse loads or the θ is relatively large (Lian *et al.* 2016). We here gave up the so-called small-rotation-angle assumption and took into account the initial stress in membrane, and presented the closed-form solution of the problem dealt with here. The presented numerical examples show this closed-form solution has higher calculation accuracy and can be applied for a wider range in comparison with the existing approximate solution, as will be seen later. Moreover, some important issues were further discussed based on the numerical examples.

2. Membrane equation and its solution

An initially flat elastic circular membrane is extended a radial plane displacement u_0 at the perimeter of radius a, and then is fixed at the perimeter of radius a. A circular membrane structure with initial stress is thus modelled. A uniformly-distributed transverse loads q is quasi-statically applied onto the membrane surface, and when the loads q reaches a large enough value the deflected membrane will get in contact with a frictionless rigid plate being parallel to the initially flat membrane, as shown in Fig. 1, where r is the radial coordinate, w is the transversal displacement, b is the radius of the membrane contacting with the horizontal frictionless rigid plate, and g is the gap between the horizontal frictionless rigid plate and the initially flat membrane.

Such a problem can be viewed as consisting of two local membrane problems in the central portion of $0<r\le b$ and in the annular portion of $b\le r\le a$, which are connected by the continuity conditions at $r=b$. The problem in $0<r\le b$ may be simplified as a plane tension problem of membrane, while the problem in $b<r\le a$ is still the one of membrane deflection. As for the case before contact between the deformed membrane and the horizontal frictionless rigid plate, the well-known Hencky problem, it has been dealt with and its solution may be found in Lian *et al.* (2016).

In the annular portion, let us take a piece of the central portion of the annular membrane whose radius is r ($b\le r\le a$) to study the static problem of equilibrium of this membrane, as shown in Fig. 2, where σ_r is the radial stress, h is the thickness and θ is the slope angle of membrane. Right here there are three vertical forces, i.e., total force $\pi r^2 q$ (in which $b\le r\le a$) of the uniformly-distributed loads q, total reaction force $\pi b^2 q$ from the rigid plate, and total vertical force $2\pi r\sigma_r h\sin\theta$ produced by the membrane force $\sigma_r h$. The out-plane equilibrium equation is

$$2\pi r\sigma_r h\sin\theta = \left(\pi r^2 - \pi b^2\right)q, \tag{1}$$

where

$$\sin\theta = 1\Big/\sqrt{1+1/\tan^2\theta} = 1\Big/\sqrt{1+1/(-\mathrm{d}w/\mathrm{d}r)^2}. \tag{2}$$

Substituting Eq. (2) into Eq. (1), one has

$$2r\sigma_r h = q\left(r^2 - b^2\right)\sqrt{1+1/(-\mathrm{d}w/\mathrm{d}r)^2}. \tag{3}$$

The in-plane equilibrium equation is

$$\frac{\mathrm{d}}{\mathrm{d}r}(r\sigma_r h) - \sigma_t h = 0, \tag{4}$$

where σ_t is the circumferential stress. The relations of strain and displacement of the large deflection problem are

$$e_r = \frac{\mathrm{d}u}{\mathrm{d}r} + \frac{1}{2}\left(\frac{\mathrm{d}w}{\mathrm{d}r}\right)^2,\ e_t = \frac{u}{r}, \tag{5a, b}$$

where e_r is the radial strain, e_t is the circumferential strain, and u is the radial displacement. The relations of stress and strain are

$$\sigma_r = \frac{E}{1-\nu^2}(e_r + \nu e_t),\ \sigma_t = \frac{E}{1-\nu^2}(e_t + \nu e_r), \tag{6a, b}$$

where E and ν denote the Young's modulus of elasticity and Poisson's ratio of membrane, respectively. Substituting Eq. (5) into Eq. (6),

$$\begin{aligned}\sigma_r &= \frac{E}{1-\nu^2}\left[\frac{\mathrm{d}u}{\mathrm{d}r} + \frac{1}{2}\left(\frac{\mathrm{d}w}{\mathrm{d}r}\right)^2 + \nu\frac{u}{r}\right],\\ \sigma_t &= \frac{E}{1-\nu^2}\left[\frac{u}{r} + \nu\frac{\mathrm{d}u}{\mathrm{d}r} + \frac{\nu}{2}\left(\frac{\mathrm{d}w}{\mathrm{d}r}\right)^2\right].\end{aligned} \tag{7a, b}$$

By means of Eqs. (4) and (7), one has

$$\frac{u}{r} = \frac{1}{E}(\sigma_t - \nu\sigma_r) = \frac{1}{E}\left[\frac{\mathrm{d}}{\mathrm{d}r}(r\sigma_r) - \nu\sigma_r\right]. \tag{8}$$

If we substitute the u of Eq. (8) into Eq. (7a), the compatibility equation may be written as

$$r\frac{\mathrm{d}}{\mathrm{d}r}\left[\frac{1}{r}\frac{\mathrm{d}}{\mathrm{d}r}(r^2\sigma_r)\right] + \frac{E}{2}\left(\frac{\mathrm{d}w}{\mathrm{d}r}\right)^2 = 0. \tag{9}$$

In the central portion ($0<r\le b$), noting that $dw/dr=0$, from Eq. (5) it may be found that

$$e_r = \frac{\mathrm{d}u}{\mathrm{d}r},\ e_t = \frac{u}{r}. \tag{10a, b}$$

Substituting Eq. (10) into Eq. (6),

$$\sigma_r = \frac{E}{1-\nu^2}\left(\frac{\mathrm{d}u}{\mathrm{d}r} + \nu\frac{u}{r}\right), \sigma_t = \frac{E}{1-\nu^2}\left(\frac{u}{r} + \nu\frac{\mathrm{d}u}{\mathrm{d}r}\right). \quad (11a, b)$$

Substituting Eq. (11) into Eq. (4), one has

$$r\frac{\mathrm{d}^2 u}{\mathrm{d}r^2} + \frac{\mathrm{d}u}{\mathrm{d}r} - \frac{u}{r} = 0. \quad (12)$$

Under the conditions

$$u = 0 \text{ at } r = 0 \text{ and } u = u(b) \text{ at } r = b, \quad (13a, b)$$

the solution of Eq. (12) may be written as

$$u(r) = \frac{u(b)}{b}r. \quad (14)$$

So, substituting Eq. (14) into Eqs. (10) and (11), it is found that

$$e_r = e_t = \frac{u(b)}{b} \text{ and } \sigma_r = \sigma_t = \frac{E}{1-\nu}\frac{u(b)}{b} \quad \text{in } 0 \le r \le b. \quad (15a, b)$$

So, the boundary conditions and continuous conditions are

$$w = 0 \text{ and } \frac{u}{r} = \frac{u_0}{a} = \frac{1-\nu}{E}\sigma_0 \text{ at } r = a \quad (16a, b)$$

and

$$w = g, \left(\frac{u}{r}\right)_B = \left(\frac{u}{r}\right)_A = \frac{u(b)}{b} \text{ and } (\sigma_r)_B = (\sigma_r)_A = \frac{E}{1-\nu}\frac{u(b)}{b} \text{ at } r = b, \quad (17a, b, c)$$

where σ_0 is the initial stress in membrane, the subscript A and B denote the values of various variables on two sides of the inter-connecting circle, the side of region (A) is the section whose deflection is restricted, and the side of region (B) is not.

Let us introduce the following nondimensional variables

$$Q = \frac{qa}{Eh}, W = \frac{w}{a}, S_r = \frac{\sigma_r}{E}, S_t = \frac{\sigma_t}{E}, S_0 = \frac{\sigma_0}{E}, x = \frac{r}{a}, \alpha = \frac{b}{a}, \quad (18)$$

and transform Eqs. (3), (9), (8), (16a, b) and (17a, b, c) into

$$\left(\frac{\mathrm{d}W}{\mathrm{d}x}\right)^2 = \frac{Q^2(x^2-\alpha^2)^2}{4x^2S_r^2 - Q^2(x^2-\alpha^2)^2}, \quad (19)$$

$$x^2\frac{\mathrm{d}^2 S_r}{\mathrm{d}x^2} + 3x\frac{\mathrm{d}S_r}{\mathrm{d}x} + \frac{1}{2}\left(\frac{\mathrm{d}W}{\mathrm{d}x}\right)^2 = 0, \quad (20)$$

$$\frac{u}{r} = (1-\nu)S_r + x\frac{\mathrm{d}S_r}{\mathrm{d}x}, \quad (21)$$

$$W = 0 \text{ and } \frac{u}{r} = (1-\nu)S_0 \text{ at } x = 1, \quad (22)$$

and

$$W = \frac{g}{a}, \left(\frac{u}{r}\right)_B = \left(\frac{u}{r}\right)_A = \frac{u(b)}{b} \text{ and } (S_r)_B = (S_r)_A = \frac{1}{1-\nu}\frac{u(b)}{b} \text{ at } x = \alpha. \quad (23a, b, c)$$

Letting β=(1+α)/2 and expanding S_r and W into the power series in powers of x–β, i.e., letting

$$S_r = \sum_{i=0}^{\infty} c_i(x-\beta)^i \quad (24)$$

and

$$W = \sum_{i=0}^{\infty} d_i(x-\beta)^i. \quad (25)$$

After substituting Eqs. (24) and (25) into Eqs. (19) and (20), the coefficients c_i(i=2,3,4…) and d_i(i=1,2,3…) can be expressed by the polynomial of c_0 and c_1, which are shown in Appendixes A and B, respectively. The coefficients c_0, c_1 and d_0 are left as undetermined constants and they can be determined by using the boundary conditions and continuous conditions as follows.

From Eq (25), Eqs. (22a) and (23a) give

$$\sum_{i=0}^{\infty} d_i(1-\beta)^i = 0 \quad (26)$$

and

$$\sum_{i=0}^{\infty} d_i(\alpha-\beta)^i = \frac{g}{a}. \quad (27)$$

From Eqs. (21) and (24), Eqs. (22b) and (23b) give

$$(1-\nu)\sum_{i=0}^{\infty} c_i(1-\beta)^i + \sum_{i=1}^{\infty} ic_i(1-\beta)^{i-1} = (1-\nu)S_0 \quad (28)$$

and

$$(1-\nu)\sum_{i=0}^{\infty} c_i(\alpha-\beta)^i + \alpha\sum_{i=1}^{\infty} ic_i(\alpha-\beta)^{i-1} = \frac{u(b)}{b}. \quad (29)$$

From Eq. (24), Eq. (23c) gives

$$\sum_{i=0}^{\infty} c_i(\alpha-\beta)^i = \frac{1}{1-\nu}\frac{u(b)}{b}. \quad (30)$$

Eliminating the $u(b)$ from Eqs. (29) and (30), one has

$$\sum_{i=1}^{\infty} ic_i(\alpha-\beta)^{i-1} = 0. \quad (31)$$

Hence, for the given problem where a, h, g, E, ν, q and σ_0 are known in advance, the contact radius b and the undetermined constants, c_0, c_1 and d_0 can be determined by Eqs. (26), (27), (28) and (31), consequently the coefficients c_i(i=2,3,4…) and d_i(i=1,2,3…) can be determined. Finally, the problem considered here can thus be dealt with.

3. Results and discussions

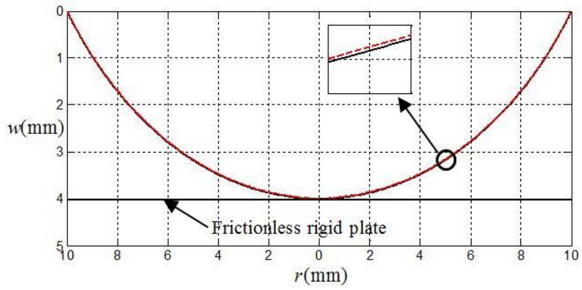

Fig. 3 Variation of w with r when q takes 0.214 MPa

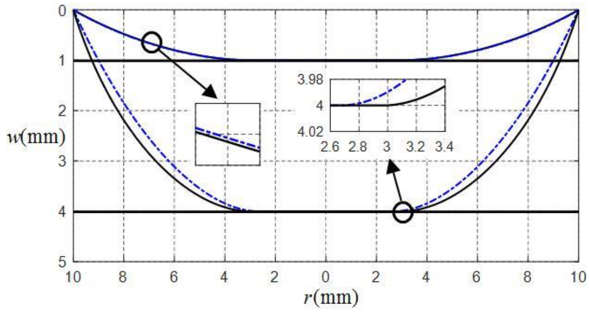

Fig. 4 Variation of w with r when g takes 1 mm and 4 mm

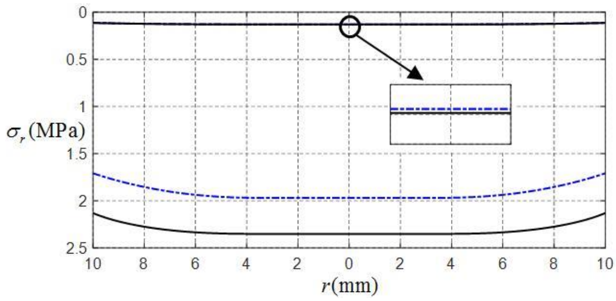

Fig. 5 Variation of σ_r with r when g takes 1 mm and 4 mm

By giving up the small-rotation-angle assumption and taking into account the initial stress, the closed-form solution presented above has higher calculation accuracy and wider application range in comparison with the existing approximate solution. Now, let us consider a circular rubber film with a=10 mm, h=1 mm, E=7.84 MPa, and v=0.47 to demonstrate the validity of the solution presented here and discuss the influence of the small-rotation-angle assumption and the initial stress based on the results of numerical calculations.

We here use the existing mature theory (solution in Lian *et al.* 2017) to examine the reliability of the closed-form solution presented here. Apparently, when σ_0=0 MPa and $b\rightarrow0$, the numerical calculation results obtained by the solution presented here should be close to the results obtained by the solution presented in Lian *et al.* (2017). Fig. 3 shows the variation of w with r while g=4 mm, σ_0=0 MPa and q=0.214 MPa, where the solid line represents the results obtained by the solution presented here (the corresponding b is 0.001 mm), and the dashed line by the solution presented in Lian *et al.* (2017). From Fig. 3 it may be seen that the two profiles $w(r)$ are very close to each other, which shows that, to some extent, the closed-form solution presented here is reliable.

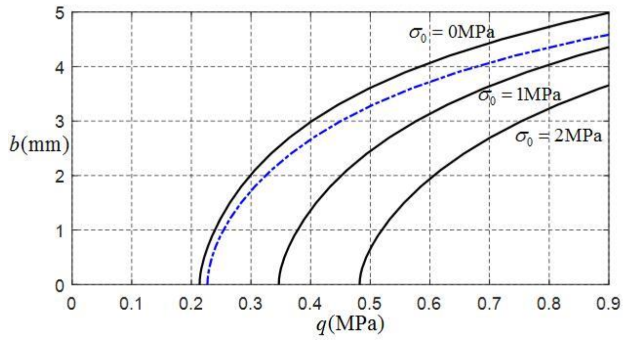

Fig. 6 Variation of b with q when σ_0 takes 0 MPa, 1 MPa and 2 MPa

Let us show the effect of giving up the small-rotation-angle assumption by comparing the results obtained by the solution without the small-rotation-angle assumption (presented here) and the solution with the small-rotation-angle assumption (presented in Wang *et al.* 2018). Figs. 4 and 5 show the variation of w and σ_r with r when g=1 mm (q=0.007 MPa) and g=4 mm (q=0.402 MPa), respectively, where the solid line represents the results obtained by the solution presented here (in which σ_0=0 MPa), and the dot and dash line by the solution presented in Wang *et al.* (2018). From Figs. 4 and 5 it can be seen that, when the slope angle θ of membrane is relatively small (i.e., when g=1 mm), the solid lines are very close to the dot and dash lines, which also shows that the closed-form solution presented here is reliable. But when the slope angle θ of membrane is relatively large (i.e., when g=4 mm), the contact radius b of the solid line is 3 mm but the dot and dash line is 2.68 mm, moreover, the difference between the solid lines and the dot and dash lines is also obvious. These differences are mainly caused by the small-rotation-angle assumption adopted in Wang *et al.* (2018).

Fig. 6 shows the variation of b with q when σ_0 takes 0 MPa, 1 MPa and 2 MPa, respectively, where the solid lines represent the results obtained by the solution presented here, and the dot and dash line by the solution presented in Wang *et al.* (2018). From Fig. 6 it may be seen that, under the same applied loads q, the initial stress σ_0 will reduce the contact radius b, and that is to say, to achieve the same contact radius, greater applied loads is required with the increases of the initial stress. In addition, when σ_0 takes 0MPa, the difference between the dot and dash line and the solid line increases with the increase of the applied loads, which is also caused by the small-rotation-angle assumption adopted in Wang *et al.* (2018).

4. Conclusions

In this study, we analytically solved the problem of axisymmetric deformation of prestressed Föppl-Hencky membrane under constrained deflecting, in which the small-rotation-angle assumption usually adopted in membrane problems was given up and the initial stress in membrane was considered. The comparisons with existing solutions verified the validity of this work. The following main conclusions can be drawn:

(i) When the deformation of the membrane increases further, the error due to the adoption of small-rotation-angle assumption will increase accordingly, this makes the solution presented in our study more competitive.

(ii) The introduction of initial stress has effect on the contact radius in such a constrained deflecting problem. Under the same magnitude of applied loads, the greater the initial stress, the smaller the contact radius.

(iii) There is no doubt that, by giving up small-rotation-angle assumption and also incorporating the initial stress, the application scope of solution obtained here has been improved further.

This work will be helpful in the design of the touch mode capacitive pressure sensors, and in the synchronous characterization of the mechanical properties of thin films. Especially, when the thin film is very flexible, the large-rotation-angle deformations will inevitable be introduced, which makes the influence of the initial stress on deformation has to be further considered in this case.

Acknowledgements

This work was funded by the National Natural Science Foundation of China (Grant No. 11772072).

References

Alekseev, S.A. (1953), "Elastic circular membranes under the uniformly distributed loads", *Eng. Corp.*, **14**, 196-198.

Arthurs, A.M. and Clegg, J. (1994), "On the solution of a boundary value problem for the nonlinear Föppl-Hencky equation", *Z. Angew. Math. Mech.*, **74**(7), 281-284.

Beck, A. and Grabmuller, H. (1992), "Wrinkle-free solutions of circular membrane problems", *Z. Angew. Math. Phys.*, **43**(3), 481-504.

Chien, W.Z. (1948), "Asymptotic behavior of a thin clamped circular plate under uniform normal pressure at very large deflection", *Sci. Rep. Nat. Tsinghua Univ.*, **5**(1), 193-208.

Chucheepsakul, S., Kaewunruen, S. and Suwanarat, A. (2009), "Large deflection analysis of orthotropic, elliptic membranes", *Struct. Eng. Mech.*, **31**(6), 625-638.

Ersoy, H., Ozpolat, L. and Civalek, O. (2009), "Free vibration of circular and annular membranes with varying density by the method of discrete singular convolution", *Struct. Eng. Mech.*, **32**(5), 621-634.

Feng, L.Y., Li, X.W. and Shi, T.L. (2015), "Nonlinear large deflection of thin film overhung on compliant substrate using shaft-loaded blister test", *J. Appl. Mech.*, **82**(9), 091001.

Hasheminejad, S.M. and Ghaheri, A. (2015), "Exact solution for vibration analysis of an eccentric elliptical membrane", *Z. Angew. Math. Mech.*, **95**(7), 730-741.

Hencky, H. (1915), "Über den spannungszustand in kreisrunden platten mit verschwindender biegungssteifigkeit", *Zeitschrift Für Mathematik und Physik*, **63**, 311-317.

Lian, Y.S., He, X.T., Liu, G.H., Sun, J.Y. and Zheng, Z.L. (2017a), "Application of perturbation idea to well-known Hencky problem: A perturbation solution without small-rotation-angle assumption", *Mech. Res. Commun.*, **83**(7), 32-46.

Lian, Y.S., Sun, J.Y., Ge, X.M., Yang, Z.X., He, X.T. and Zheng, Z.L. (2017b), "A theoretical study of an improved capacitive pressure sensor: Closed-form solution of uniformly loaded annular membranes", *Measurement*, **111**, 84-92.

Lian, Y.S., Sun, J.Y., Yang, Z.X., He, X.T. and Zheng, Z.L. (2016), "Closed-form solution of well-known Hencky problem without small-rotation-angle assumption", *Z. Angew. Math. Mech.*, **96**(12), 1434-1441.

Molla-Alipour, M. and Ganji, B.A. (2015), "Analytical analysis of mems capacitive pressure sensor with circular diaphragm under dynamic load using differential transformation method (DTM)", *Acta Mech. Sol. Sin.*, **28**(4), 400-408.

Sun, J.Y., Hu, J.L., He, X.T. and Zheng, Z.L. (2010), "A theoretical study of a clamped punch-loaded blister configuration: The quantitative relation of load and deflection", *Int. J. Mech. Sci.*, **52**(7), 928-936.

Sun, J.Y., Hu, J.L., Zheng, Z.L., He, X.T. and Geng, H.H. (2011), "A practical method for simultaneous determination of Poisson's ratio and Young's modulus of elasticity of thin films", *J. Mech. Sci. Technol.*, **25**(12), 3165-3171.

Sun, J.Y., Lian, Y.S., Li, Y.M., He, X.T. and Zheng, Z.L. (2015), "Closed-form solution of elastic circular membrane with initial stress under uniformly-distributed loads: Extended Hencky solution", *Z. Angew. Math. Mech.*, **95**(11), 1335-1341.

Sun, J.Y., Lian, Y.S., Li, Z.L., He, X.T. and Zheng, Z.L. (2014), "Theoretical study on shaft-loaded blister test technique: Synchronous characterization of surface and interfacial mechanical properties", *Int. J. Adhes. Adhes.*, **51**, 128-139.

Sun, J.Y., Rong, Y., He, X.T., Gao, X.W. and Zheng, Z.L. (2013), "Power series solution of circular membrane under uniformly distributed loads: Investigation into Hencky transformation", *Struct. Eng. Mech.*, **45**(5), 631-641.

Todorovic, D.M., Rabasovic, M.D., Markushev, D.D. and Sarajlic, M. (2014), "Photoacoustic elastic bending in thin film-substrate system: Experimental determination of the thin film parameters", *J. Appl. Phys.*, **116**(5), 273-318.

Wang, T.F., He, X.T. and Li, Y.H. (2018), "Closed-form solution of a peripherally fixed circular membrane under uniformly-distributed transverse loads and deflection restrictions", *Math. Probl. Eng.*, 5989010.

Weinitschke, H.J. (1973), "Endliche deformationen elastischer membranen", *Z. Angew. Math. Mech.*, **53**(12), T89-T90.

Yang, Z.X., Sun, J.Y., Li, K., Lian, Y.S., He, X.T. and Zheng, Z.L. (2018), "Theoretical study on synchronous characterization of surface and interfacial mechanical properties of thin-film-substrate systems with residual stress based on pressure blister test technique", *Polymers*, **10**(1), 49.

Yang, Z.X., Sun, J.Y., Ran, G.M. and He, X.T. (2017), "A new solution to Föppl-Hencky membrane equation", *J. Mech.*, **33**(4), N7-N11.

CC

Appendix A

$$c_2=-\frac{1}{4}\frac{6Q^2\beta e^2c_1-24\beta^3c_0^2c_1-Q^2e^2}{(Q^2e^2-4\beta^2c_0^2)\beta^2},$$

$$\begin{aligned}c_3=&\frac{1}{12\beta^3(Q^2e^2-4\beta^2c_0^2)^2}(24Q^4\beta e^4c_1-192Q^2\beta^3e^2c_0{}^2c_1-5Q^4e^4\\&+384\beta^5c_0{}^4c_1-16Q^2\beta^4ec_0{}^2+8Q^2\beta^3e^2c_0c_1+28Q^2\beta^2e^2c_0{}^2),\end{aligned}$$

$$\begin{aligned}c_4=&-\frac{1}{48\beta^4(Q^2e^2-4\beta^2c_0^2)^3}(120Q^6\beta e^6c_1-96Q^4\beta^6e^2c_0{}^2\\&+64Q^4\beta^5e^3c_0c_1-8Q^4\beta^4e^4c_1{}^2-1440Q^4\beta^3e^4c_0{}^2c_1\\&-128Q^2\beta^8c_0{}^4+256Q^2\beta^7ec_0{}^3c_1-96Q^2\beta^6e^2c_0{}^2c_1{}^2\\&-7680\beta^7c_0{}^6c_1+5760Q^2\beta^5e^2c_0{}^4c_1-32Q^4\beta^4e^3c_0{}^2-27Q^6e^6\\&+48Q^4\beta^3e^4c_0c_1+640Q^2\beta^6ec_0{}^4-448Q^2\beta^5e^2c_0{}^3c_1\\&+264Q^4\beta^2e^4c_0{}^2-752Q^2\beta^4e^2c_0{}^4-4Q^4\beta^2e^4c_0),\end{aligned}$$

$$\begin{aligned}c_5=&\frac{1}{60\beta^5(Q^2e^2-4\beta^2c_0^2)^4}(-192Q^6\beta^8e^3c_0{}^2+144Q^6\beta^7e^4c_0c_1\\&-24Q^6\beta^6e^5c_1{}^2-768Q^4\beta^{10}ec_0{}^4+1536Q^4\beta^9e^2c_0{}^3c_1\\&-768Q^4\beta^8e^3c_0{}^2c_1{}^2+96Q^4\beta^7e^4c_0c_1{}^3+768Q^2\beta^{11}c_0{}^5c_1\\&-1152Q^2\beta^{10}ec_0{}^4c_1{}^2+384Q^2\beta^9e^2c_0{}^3c_1{}^3+180Q^8\beta e^8c_1\\&+96Q^6\beta^5e^5c_0c_1-24Q^6\beta^4e^6c_1{}^2-2880Q^6\beta^3e^6c_0{}^2c_1\\&+1920Q^4\beta^8e^2c_0{}^4-1536Q^4\beta^7e^3c_0{}^3c_1+96Q^4\beta^6e^4c_0{}^2c_1{}^2\\&+17280Q^4\beta^5e^4c_0{}^4c_1+1536Q^2\beta^{10}c_0{}^6-4608Q^2\beta^9ec_0{}^5c_1\\&+2304Q^2\beta^8e^2c_0{}^4c_1{}^2-46080Q^2\beta^7e^2c_0{}^6c_1-60Q^6\beta^4e^5c_0{}^2\\&+46080\beta^9c_0{}^8c_1+78Q^6\beta^3e^6c_0c_1+480Q^4\beta^6e^3c_0{}^4\\&-1008Q^4\beta^5e^4c_0{}^3c_1-5568Q^2\beta^8ec_0{}^6+5088Q^2\beta^7e^2c_0{}^5c_1\\&-42Q^8e^8-12Q^6\beta^4e^5c_0+3Q^6\beta^3e^6c_1+582Q^6\beta^2e^6c_0{}^2\\&-64Q^4\beta^6e^3c_0{}^3+44Q^4\beta^5e^4c_0{}^2c_1-2832Q^4\beta^4e^4c_0{}^4\\&+5472Q^2\beta^6e^2c_0{}^6-8Q^6\beta^2e^6c_0+88Q^4\beta^4e^4c_0{}^3),\end{aligned}$$

$$\begin{aligned}c_6=&-\frac{1}{720\beta^6(Q^2e^2-4\beta^2c_0^2)^5}(-3840Q^8\beta^{10}e^4c_0{}^2+3072Q^8\beta^9e^5c_0c_1-3Q^8\beta^2e^8\\&-576Q^8\beta^8e^6c_1{}^2-12288Q^4\beta^{14}c_0{}^6-30720Q^6\beta^{12}e^2c_0{}^4+61440Q^6\beta^{11}e^3c_0{}^3c_1\\&-34560Q^6\beta^{10}e^4c_0{}^2c_1{}^2+6144Q^6\beta^9e^5c_0c_1{}^3+98304Q^4\beta^{13}ec_0{}^5c_1-138240Q^4\beta^{12}e^2c_0{}^4c_1{}^2\\&+1440Q^8\beta^5e^7c_0c_1+61440Q^4\beta^{11}e^3c_0{}^3c_1{}^3-7680Q^4\beta^{10}e^4c_0{}^2c_1{}^4-36864Q^2\beta^{14}c_0{}^6c_1{}^2\\&+49152Q^2\beta^{13}ec_0{}^5c_1{}^3-15360Q^2\beta^{12}e^2c_0{}^4c_1{}^4+1152Q^8\beta^8e^5c_0{}^2+1440Q^8\beta^7e^6c_0c_1\\&-624Q^8\beta^6e^7c_1{}^2-192Q^6\beta^8e^6c_1{}^4+61440Q^6\beta^{10}e^3c_0{}^4-51840Q^6\beta^9e^4c_0{}^3c_1\\&+960Q^6\beta^8e^5c_0{}^2c_1{}^2+2496Q^6\beta^7e^6c_0c_1{}^3-373248Q^4\beta^{11}e^2c_0{}^5c_1+234240Q^4\beta^{10}e^3c_0{}^4c_1{}^2\\&-30720Q^4\beta^9e^4c_0{}^3c_1{}^3-50400Q^8\beta^3e^8c_0{}^2c_1-129024Q^2\beta^{13}c_0{}^7c_1+267264Q^2\beta^{12}ec_0{}^6c_1{}^2\\&-113664Q^2\beta^{11}e^2c_0{}^5c_1{}^3+2520Q^{10}\beta e^{10}c_1-720Q^8\beta^6e^6c_0{}^2+1440Q^8\beta^5e^7c_0c_1\\&-492Q^8\beta^4e^8c_1{}^2-6720Q^6\beta^8e^4c_0{}^4-21120Q^6\beta^7e^5c_0{}^3c_1+403200Q^6\beta^5e^6c_0{}^4c_1\\&-225024Q^4\beta^{10}e^2c_0{}^6+228864Q^4\beta^9e^3c_0{}^5c_1+1888Q^6\beta^4e^6c_0{}^3+129024Q^4\beta^{12}ec_0{}^6\\&-6720Q^4\beta^8e^4c_0{}^4c_1{}^2-1612800Q^4\beta^7e^4c_0{}^6c_1-125952Q^2\beta^{12}c_0{}^8+509952Q^2\beta^{11}ec_0{}^7c_1\\&-324864Q^2\beta^{10}e^2c_0{}^6c_1{}^2+3225600Q^2\beta^9e^2c_0{}^8c_1-44Q^6\beta^4e^6c_0{}^2-2580480\beta^{11}c_0{}^{10}c_1\\&-288Q^8\beta^6e^6c_0-600Q^{10}e^{10}-840Q^8\beta^4e^7c_0{}^2-11424Q^4\beta^6e^4c_0{}^5+5520Q^6\beta^6e^6c_0{}^2c_1{}^2\\&+1140Q^8\beta^3e^8c_0c_1-3776Q^6\beta^8e^4c_0{}^3+3584Q^6\beta^7e^5c_0{}^2c_1-50400Q^8\beta^3e^8c_0{}^2c_1\\&-492Q^8\beta^4e^8c_1{}^2+13920Q^6\beta^6e^5c_0{}^4-19440Q^6\beta^5e^6c_0{}^3c_1-3840Q^4\beta^{10}e^2c_0{}^5\\&+7680Q^4\beta^9e^3c_0{}^4c_1-3264Q^4\beta^8e^4c_0{}^3c_1{}^2-43392Q^4\beta^8e^3c_0{}^6+123840Q^4\beta^7e^4c_0{}^5c_1\\&+397824Q^2\beta^{10}ec_0{}^8-453888Q^2\beta^9e^2c_0{}^7c_1-184Q^8\beta^4e^7c_0+10740Q^8\beta^2e^8c_0{}^2\\&+94Q^8\beta^3e^8c_1+3168Q^6\beta^6e^5c_0{}^3-320Q^6\beta^5e^6c_0{}^2c_1-74160Q^6\beta^4e^6c_0{}^4+96Q^8\beta^5e^7c_1\\&+13824Q^4\beta^8e^3c_0{}^5-12000Q^4\beta^7e^4c_0{}^4c_1+239040Q^4\beta^6e^4c_0{}^6-352512Q^2\beta^8e^2c_0{}^8\\&-126Q^8\beta^2e^8c_0-373248Q^4\beta^{11}e^2c_0{}^5c_1+234240Q^4\beta^{10}e^3c_0{}^4c_1{}^2-30720Q^4\beta^9e^4c_0{}^3c_1{}^3\\&-129024Q^2\beta^{13}c_0{}^7c_1+267264Q^2\beta^{12}ec_0{}^6c_1{}^2-113664Q^2\beta^{11}e^2c_0{}^5c_1{}^3-656Q^6\beta^6e^6c_0c_1{}^2\\&-6720Q^6\beta^8e^4c_0{}^4-21120Q^6\beta^7e^5c_0{}^3c_1+5520Q^6\beta^6e^6c_0{}^2c_1{}^2+403200Q^6\beta^5e^6c_0{}^4c_1\\&-225024Q^4\beta^{10}e^2c_0{}^6+228864Q^4\beta^9e^3c_0{}^5c_1-11424Q^4\beta^6e^4c_0{}^5-6720Q^4\beta^8e^4c_0{}^4c_1{}^2\\&-1612800Q^4\beta^7e^4c_0{}^6c_1-125952Q^2\beta^{12}c_0{}^8+1888Q^6\beta^4e^6c_0{}^3+509952Q^2\beta^{11}ec_0{}^7c_1\\&-324864Q^2\beta^{10}e^2c_0{}^6c_1{}^2+3225600Q^2\beta^9e^2c_0{}^8c_1+2520Q^{10}\beta e^{10}c_1-2580480\beta^{11}c_0{}^{10}c_1\\&-288Q^8\beta^6e^6c_0+96Q^8\beta^5e^7c_1-840Q^8\beta^4e^7c_0{}^2-44Q^6\beta^4e^6c_0{}^2+1140Q^8\beta^3e^8c_0c_1\\&-3776Q^6\beta^8e^4c_0{}^3+3584Q^6\beta^7e^5c_0{}^2c_1-656Q^6\beta^6e^6c_0c_1{}^2-720Q^8\beta^6e^6c_0^2-3Q^8\beta^2e^8\\&+13920Q^6\beta^6e^5c_0{}^4-19440Q^6\beta^5e^6c_0{}^3c_1-3840Q^4\beta^{10}e^2c_0{}^5+7680Q^4\beta^9e^3c_0{}^4c_1\\&-3264Q^4\beta^8e^4c_0{}^3c_1{}^2-43392Q^4\beta^8e^3c_0{}^6+123840Q^4\beta^7e^4c_0{}^5c_1+397824Q^2\beta^{10}ec_0{}^8\\&-453888Q^2\beta^9e^2c_0{}^7c_1-600Q^{10}e^{10}-184Q^8\beta^4e^7c_0+94Q^8\beta^3e^8c_1+10740Q^8\beta^2e^8c_0{}^2\\&+3168Q^6\beta^6e^5c_0{}^3-320Q^6\beta^5e^6c_0{}^2c_1-74160Q^6\beta^4e^6c_0{}^4+13824Q^4\beta^8e^3c_0{}^5\\&-12000Q^4\beta^7e^4c_0{}^4c_1+239040Q^4\beta^6e^4c_0{}^6-352512Q^2\beta^8e^2c_0{}^8-126Q^8\beta^2e^8c_0)\end{aligned}$$

where $e=\beta^2-\alpha^2$.

Appendix B

$$d_1=-\frac{eQ}{(4\beta^2c_0^2-e^2Q^2)^{1/2}},$$

$$d_2=-\frac{2Q\beta c_0(2\beta^2c_0-\beta ec_1-ec_0)}{(4\beta^2c_0^2-e^2Q^2)^{3/2}},$$

$$\begin{aligned}d_3=&\frac{Q}{3(4\beta^2c_0^2-e^2Q^2)^{5/2}}(e^3Q^2c_0+2e^3Q^2c_0^2-20e^2Q^2\beta^2c_0^2\\&+24eQ^2\beta^4c_0^2+16e\beta^2c_0^4-16\beta^4c_0^4+2e^3Q^2\beta c_0c_1-32\beta^5c_0^3c_1\\&-16e^2Q^2\beta^3c_0c_1+40e\beta^3c_0^3c_1+2e^3Q^2\beta^2c_1^2+16e\beta^4c_0^2c_1^2),\end{aligned}$$

$$\begin{aligned}d_4=&\frac{Q}{12\beta(4\beta^2c_0^2-e^2Q^2)^{7/2}}\{192\beta^4(e-\beta^2)c_0^6+96\beta^5(9e\\&-8\beta^2)c_0^5c_1+3e^4Q^4\beta c_1[e-2\beta(e+4\beta^2)c_1]-8e^2Q^2\beta^2c_0^2\\&\times[3Q^2(2e^2-9e\beta^2+8\beta^4)-4e\beta c_1+(66\beta^4-24e\beta^2)c_1^2]\\&+24c_0^4[Q^2\beta^2(3e^3-20e^2\beta^2+24e\beta^4-8\beta^6)+16(2e\beta^6\\&-\beta^8)c_1^2]+8e\beta^2c_0^3[5eQ^2(e-\beta^2)+6Q^2\beta(3e^2-22e\beta^2\\&+18\beta^4)c_1+24\beta^5c_1^3]+e^3Q^2c_0[eQ^2(e-12\beta^2)\\&-48Q^2\beta^3(e-3\beta^2)c_1+72\beta^5c_1^3]\},\end{aligned}$$

$$\begin{aligned}d_5=&-\frac{Q}{120\beta^2(4\beta^2c_0^2-e^2Q^2)^{9/2}}\{6144\beta^6(e-\beta^2)c_0^8+3072\beta^7(14e\\&-13\beta^2)c_0^7c_1+768\beta^4c_0^6[3Q^2(2e^3-11e^2\beta^2+13e\beta^4-4\beta^6)\\&+(82e\beta^4-56\beta^6)c_1^2]-2e^4Q^4c_0[eQ^2(e^2+40e\beta^2-144\beta^4)\\&+48Q^2\beta^3(e^2-18e\beta^2+32\beta^4)c_1-256e\beta^4c_1^2+144\beta^5(16\beta^2\\&+e)c_1^3]+32e^2Q^2\beta^2c_0^3[eQ^2(9e^2-81e\beta^2+76\beta^4)+9Q^2\beta(e^3\\&-46e^2\beta^2+172e\beta^4-128\beta^6)c_1+58e\beta^4c_1^2+36(17e\beta^5\\&-28\beta^7)c_1^3]+32\beta^4c_0^5[eQ^2(87e^2+40\beta^4-124e\beta^2)+36Q^2\beta\\&\times(13e^3-84e^2\beta^2+84e\beta^4-16\beta^6)c_1+96(11e\beta^5-4\beta^7)c_1^3]\\&-16e^3Q^2\beta^2c_0^2[6e^3Q^4+336eQ^4\beta^4-240Q^4\beta^6-e^2Q^2(117Q^2\beta^2\\&+2)+eQ^2\beta(-53e+164\beta^2)c_1+54Q^2\beta^2(e^2+14e\beta^2-28\beta^4)c_1^2\\&-288\beta^6c_1^4]+e^5Q^4[3e^2Q^2-4eQ^2\beta(7e+24\beta^2)c_1+12Q^2\beta^2(5e^2\\&+8e\beta^2+48\beta^4)c_1^2+144\beta^6c_1^4]+16e\beta^2c_0^4[9Q^4(e^4-44e^3\beta^2\\&+176e^2\beta^4-208e\beta^6+80\beta^8)+16eQ^2\beta^3(19e-14\beta^2)c_1\\&+36Q^2\beta^4(47e^2-180e\beta^2+96\beta^4)c_1^2+384\beta^8c_1^4]\},\end{aligned}$$

$$\begin{aligned}d_6=&-\frac{Q}{360\beta^3(4\beta^2c_0^2-e^2Q^2)^{11/2}}\{61440\beta^8(-e+\beta^2)c_0^{10}+30720\beta^9\\&\times(-20e+19\beta^2)c_0^9c_1-7680\beta^6c_0^8[Q^2(10e^3-18\beta^6-49e^2\beta^2\\&+57e\beta^4)+2(85e\beta^4-66\beta^6)c_1^2]-64\beta^6c_0^7[Q^2(777e^3-1298e^2\beta^2\\&+616e\beta^4-80\beta^6)+60Q^2\beta(95e^3-556e^2\beta^2+594e\beta^4-144\beta^6)c_1\\&+240(73e\beta^5-40\beta^7)c_1^3]-32\beta^4c_0^6[45Q^4(5e^5-118e^4\beta^2+432e^3\beta^4\\&-528e^2\beta^6+240e\beta^8-32\beta^{10})+64eQ^2\beta^3(69e^2-79e\beta^2+19\beta^4)c_1\\&+60Q^2\beta^4(451e^3-192\beta^6-1902e^2\beta^2+1440e\beta^4)c_1^2+1920\beta^8(7e\\&-2\beta^2)c_1^4]+5e^6Q^6[2e^2Q^2(e+3\beta^2)-eQ^2\beta(17e^2+32e\beta^2+144\beta^4)c_1\\&+12Q^2\beta^2(6e^2\beta^2+3e^3+64\beta^6)c_1^2-80e\beta^5c_1^3+144\beta^6(e+4\beta^2)c_1^4]\\&-2e^4Q^4\beta^2c_0^2\{60Q^2\beta^2(33e^3+1440e\beta^4-42e^2\beta^2-2176\beta^6)c_1^2\\&+Q^2[19200eQ^2\beta^6-11520Q^2\beta^8+e^3(139+1080Q^2\beta^2)-2e^2\beta^2(217\\&+4560Q^2\beta^2)]-4eQ^2\beta(201e^2+1992e\beta^2-4472\beta^4)c_1+7792e\beta^5c_1^3\\&+720(11e\beta^6-106\beta^8)c_1^4\}+16e^2Q^2\beta^4c_0^4\{2Q^2[270e^4Q^2+4320Q^2\beta^8\\&-11400eQ^2\beta^6-7e^3(8+495Q^2\beta^2)+6e^2\beta^2(8+1735Q^2\beta^2)]\\&+eQ^2\beta(-2663e^2+11864e\beta^2-7944\beta^4)c_1+180Q^2\beta^2(282e^2\beta^2\\&-780e\beta^4+3e^3+424\beta^6)c_1^2-1776e\beta^5c_1^3-960(29e\beta^6-34\beta^8)c_1^4\}\\&-32e\beta^4c_0^5[2eQ^4(183e^3-1420e^2\beta^2+1900e\beta^4-688\beta^6)+45Q^4\beta\\&\times(15e^4-396e^3\beta^2+1472e^2\beta^4-1472e\beta^6+400\beta^8)c_1+4eQ^2\beta^4\\&\times(897e-526\beta^2)c_1^2+60Q^2\beta^5(487e^2-1240e\beta^2+480\beta^4)c_1^3\\&+1920\beta^9c_1^5]-2e^5Q^4c_0\{eQ^4(e^3-10e^2\beta^2+480e\beta^4-960\beta^6)\\&+3[-2560eQ^4\beta^7+3200Q^4\beta^9+e^2(57Q^2\beta^3+360Q^4\beta^5)]c_1\\&-448eQ^2\beta^4(e+11\beta^2)c_1^2+180Q^2\beta^5(160\beta^4+3e^2)c_1^3+3600\beta^9c_1^5\}\\&-4e^3Q^2\beta^2c_0^3\{eQ^4(7e^3-2110e^2\beta^2+9040e\beta^4-7392\beta^6)+8Q^2\beta^3\\&\times[12000Q^2\beta^6-540e^3Q^2-18240eQ^2\beta^4+e^2(43+7065Q^2\beta^2)]c_1\\&+32eQ^2\beta^4(373e-699\beta^2)c_1^2-1440Q^2\beta^5(e^2+100e\beta^2-130\beta^4)c_1^3\\&+19200\beta^9c_1^5\}\}.\end{aligned}$$